

Supporting Information

Facile Engineering of TiO₂@Pd Based Hybrid Heterogeneous Nanostructures for Enhanced NO₂ Gas Sensing at Room Temperature under UV Activation

Thi Minh Thu Pham^{a#}, Kedhareswara Sairam Pasupuleti^{b#}, Tae Hyeon Jeong^{a,c}, Seung Min Lee^a, Thi Hong Men Nguyen^a, Moon-Deock Kim^{b,d*}, Young Heon Kim^{a*}

^a*Graduate School of Analytical Science and Technology (GRAST), Chungnam National University, 99 Daehak-ro, Yuseong-gu, Daejeon 34134, Republic of Korea.*

^b*Institute of Quantum Systems (IQS), Chungnam National University, 99 Daehak-ro, Yuseong-gu, Daejeon, 34134, Republic of Korea.*

^c*Center for Research Facilities, Pukyong National University, 45 Yongso-ro, Nam-gu, Busan 48513, Republic of Korea.*

^d*Department of Physics, Chungnam National University, 99 Daehak-ro, Yuseong-gu, Daejeon 34134, Republic of Korea.*

[#]These authors contributed equally to this work.

*Corresponding author. E-mail: y.h.kim@cnu.ac.kr

Synthesis mechanism of porous TiO₂@Pd Hybrid HNs formation

The formation of porous TiO₂ Ns through mesocrystals involved several steps, as follows. Initially, TBT and AA react, resulting in AA coordination to titanium centers and the formation of uncertain titanium acetate complexes ((CH₃COO)_xTi(OC₄H₉)_{4-x}) through a ligand exchange. As a byproduct of this reaction process, C₄H₉OH (butanol) was released, and the produced C₄H₉OH can react via a slow esterification reaction, resulting in water molecules. Further, when the hydrolysis-condensation and nonhydrolytic condensation processes occur, TiO₂ Ns are formed in the form of crystallized round spherical beads with soft silky fibers running along their surface with Ti-O-Ti surficial bonds. Further, the organic residuals in the as-obtained product were removed by calcination at 450 °C for 3 hours to obtain nanoporous TiO₂ Ns. This step can effectively remove any other remaining organic components and facilitate the development of a porous structure in the TiO₂ Ns.

The growth of Pd NPs on the porous TiO₂ Ns surfaces to form porous TiO₂@Pd HNs was readily achieved in aqueous medium at 90 °C using H₂PdCl₄ and LAA as the Pd precursor and mild reducing reagent, respectively. CTAB is a highly well-liked and commonly utilized stabilizing chemical for the production of hybrid structures as well as during the reduction of Pd²⁺. The use of CTAB results in the formation of single-crystalline Pd NPs encapsulating over the TiO₂ Ns surface. Further, the in-situ growth of Pd NPs on the TiO₂ Ns may cause the lattice mismatch between the two materials, resulting in more defect states that may reduce the sensing capabilities of the TiO₂@Pd HNs. To overcome this lattice mismatch and promote the growth of uniform Pd NPs, a CTAB wetting film must be established at the TiO₂ and Pd interface. Typically, this wetting film is formed by the formation of a molecular bilayer of surfactants on the surface of the seed material. Moreover, the CTAB can be used as a critical strategy for the successful growth of Pd NPs to avoid the effect of lattice mismatch between the Pd NPs and TiO₂ Ns by carefully controlling the reduction process of the metal precursors.

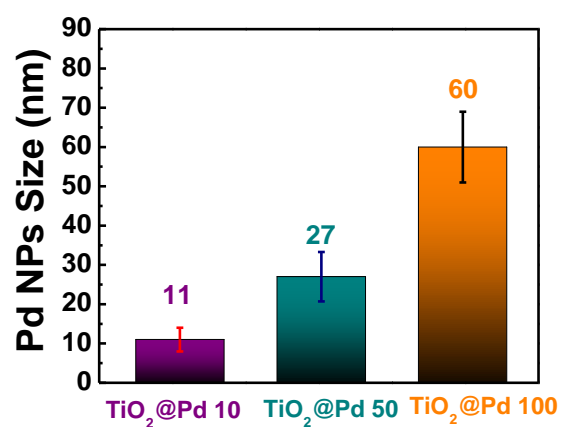


Figure S1. (a) The bar chart shows the Pd NPs size distribution over the TiO₂@Pd 10, 50, and 100 HNs samples.

Table S1. BET surface area and pore size of the as-prepared samples.

Sample	Surface area (m²/g)	Pore diameter (nm)
Bare TiO₂	86.54	13.6
TiO₂@Pd 10 HNs	129.36	15.4
TiO₂@Pd 50 HNs	164.91	21.4
TiO₂@Pd 100 HNs	156.68	20.1

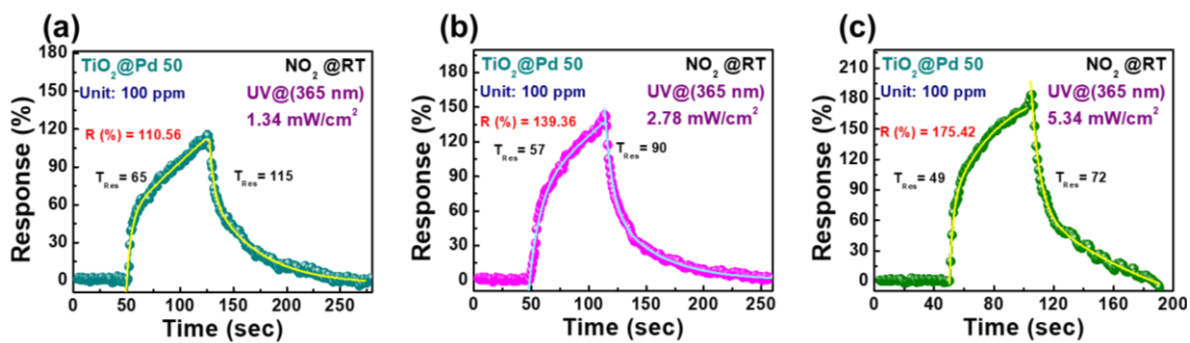


Figure S2. (a-c) The dynamic transient sensing response curves of the optimized TiO₂@Pd 50 HNs towards NO₂ (100 ppm) gas measured under different power densities (1.34, 2.78, and 5.34 mW/cm²) of UV light (365 nm) at RT.

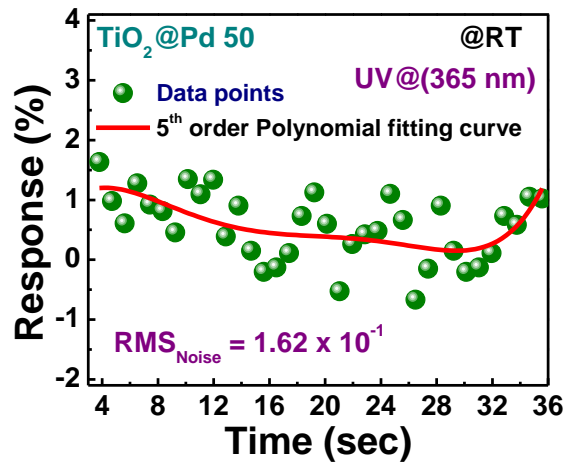


Figure S3. (a) 5th order polynomial fitting curves of the TiO₂@Pd 50 HNs sensor measured under UV@365 nm at RT (Note: the data point which we had used only the point when the sensor was in the air).

Determination of the theoretical detection limit

As per the IUPAC calculations, the theoretical detection limit (DL) of the as-prepared sensors was estimated using a well-documented formula (Eq. S1) as given below.

$$DL (ppb) = 3 \left(\frac{RMS_{noise}}{Slope} \right) \text{---} \text{---} \text{---} (S1)$$

Where the RMS_{noise} is the root mean square noise, which is estimated from the base noise level of the sensor's response/resistance points under air ambient. By using 5th-order polynomial fitting curves to the set of points displayed in Figure S2, the RMS_{noise} was calculated.

$$RMS_{noise} = \sqrt{R^2 / N} \text{---} \text{---} \text{---} (S2)$$

Here R and N were denoted as $R = \sum_{t=4}^{36} (R_i + R_f)^2 \text{---} \text{---} \text{---} (S3)$, and several points to be considered from the graph (N=32).

The slope was calculated from the linear fitting curves for the sensor's responses measured against different ppm concentration levels of the target gas. Upon substituting the slope and RMS_{noise} values in the above-mentioned equations, the calculated DL of the hybrid $TiO_2@Pd$ 50 HNs sensor was found to be 82 ppb under UV light activation. Similarly, calculations have been used to estimate the DL of the hybrid $TiO_2@Pd$ 50 HNs (DL~302 ppb) and pristine TiO_2 Ns (DL~946 ppb) sensors under dark conditions as presented in Table S2.

Table S2. Estimated detection limit TiO₂@Pd 50 hybrid HNs sensor measured under dark and UV@365 nm light illumination at RT.

S.NO	Samples	Detection limit (DL~ppb)
1.	TiO₂@Pd 50 HNs (UV (365 nm))	~82 ppb
2.	TiO₂@Pd 50 HNs (dark)	~302 ppb
3.	TiO₂ Ns	~946 ppb

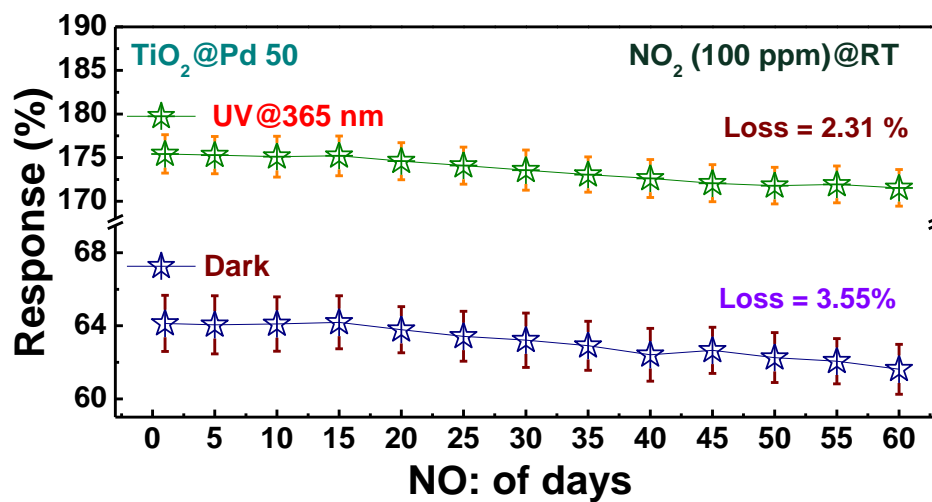


Figure S4. (a) Long-term reproducibility test results of TiO₂@Pd 50 HN sensor measured under dark and UV@365 nm light illumination towards 100 ppm of NO₂ gas at RT.